

Casting light on the 'anomalous' statistics of Mg II absorbers toward Gamma-Ray Burst afterglows: the incidence of weak systems

Nicolas Tejos¹, Sebastian Lopez¹, J. Xavier Prochaska², Joshua S. Bloom³, Hsiao-Wen Chen⁴, Miroslava Dessauges-Zavadsky⁵ and Maria J. Maureira¹

ABSTRACT

We revisit echelle spectra (spectral resolution $R \approx 40\,000$) of 8 Gamma-Ray Burst afterglows to obtain the incidence (dN/dz) of weak intervening Mg II systems at a mean redshift of $\langle z \rangle = 1.5$. We show that dN/dz of systems having restframe equivalent widths $0.07 \text{ \AA} \leq W_r^{\text{MgII}} < 1 \text{ \AA}$ toward GRBs is statistically consistent with the incidence toward QSOs. Our result is in contrast to the results for Mg II systems having $W_r \geq 1 \text{ \AA}$, where dN/dz toward GRBs has been found to be larger than toward QSOs by a factor of ≈ 4 . We confirm the overdensity albeit at a factor of ≈ 3 only. This suggests that any explanation for the GRB/QSO discrepancy, be it intrinsic to the absorbers or a selection effect, should be inherent only to the galaxies that host strong absorbers in the line-of-sight to GRBs. We argue that, of all scenarios that have been proposed, lensing amplification is the one that could explain the strong Mg II enhancement while allowing for no significant enhancement in the weak absorbers.

Subject headings: gamma rays: bursts, absorption lines, IGM

1. Introduction

The recent refinements in rapid-response spectroscopy of high-redshift Gamma-Ray Burst (GRB) optical afterglows have opened a new era in the study of the intergalactic

¹Departamento de Astronomía, Universidad de Chile, Casilla 36-D, Santiago, Chile; ntejos@das.uchile.cl

²Department of Astronomy, UCO/Lick Observatory, University of California, 1156 High Street, Santa Cruz, CA 95064

³Department of Astronomy, 601 Campbell Hall, University of California, Berkeley, CA 94720-3411

⁴Department of Astronomy, University of Chicago, 5640 S. Ellis Ave., Chicago, IL 60637

⁵Geneva Observatory, University of Geneva, 51, Ch. des Maillettes, 1290 Sauverny, Switzerland

medium (IGM, Vreeswijk et al. 2004; Fiore et al. 2005; Chen et al. 2005). In fact, using GRB afterglows instead of quasi-stellar objects (QSO) as background sources represents a superb complement to the absorption line technique in terms of redshift coverage (the highest redshift objects detected are GRBs, e.g., Olivares et al. 2009; Tanvir et al. 2009), ease of absorption system identification (no emission lines in afterglow spectra), and new insights into the interstellar medium of the host galaxies (Savaglio 2006; Prochaska et al. 2007), not to mention the novel access to the absorbers via deep imaging that the rapid fade-out of the afterglow permits (e.g., Chen et al. 2009; Pollack et al. 2009).

The first systematic, spectroscopic study of intervening systems toward GRB afterglows delivered the first surprise. Using spectra sensitive to restframe equivalent width (EW) $W_r^{2796} \geq 1 \text{ \AA}$ Mg II systems at a mean redshift of $\langle z \rangle = 1.1$, Prochter et al. (2006, hereafter P06) identified 14 such strong systems in a sample of 14 afterglow spectra at velocities $\beta c > 3000 \text{ km s}^{-1}$ from the GRB redshift. The redshift-path covered yielded almost 1 strong Mg II system per unit redshift, a roughly 4 times higher incidence than toward QSO lines-of-sight at greater than 99.9% confidence. Since the intervening absorption systems are thought to be physically independent of the background source, this result has called for a serious revision of our understanding of absorption line surveys.

Four main astrophysical effects have been proposed to explain the observed discrepancy (see P06; Porciani et al. 2007; Cucchiara et al. 2008; Sudilovsky et al. 2009): strong Mg II gas might be intrinsic to the GRB environment or host galaxy system; dust within strong Mg II absorbers might obscure faint QSOs that never get detected; GRBs might be gravitationally lensed (and amplified) by the absorbers. A fourth scenario, namely that small absorber sizes might make the distinct beam sizes of GRBs and QSOs affect the statistics differentially (Frank et al. 2007), has proven to be unviable (Pontzen et al. 2007; Thöne et al. 2008; Aoki et al. 2008). However, as argued in P06 and Porciani et al. (2007), none of these effects alone is likely to explain the QSO/GRB discrepant Mg II statistics. More recent studies have shown that the C IV statistics of QSOs and afterglows are consistent with each other (Tejos et al. 2007; Sudilovsky et al. 2007), although those surveys probed a much higher redshift and also probably different galactic environments.

In this paper we use echelle spectra of GRB afterglows, sensitive to $W_r^{2803} \geq 0.07 \text{ \AA}$, to explore the *weak* Mg II systems. The QSO Mg II EW distribution shows a clear turnover around $W_r \sim 0.3 \text{ \AA}$, hinting at different populations (e.g., Churchill et al. 1999; Nestor et al. 2005; Milutinović et al. 2006; Narayanan et al. 2007, hereafter N07). Here we show for the first time that, contrary to the strong systems, the *weak* ($W_r < 0.3 \text{ \AA}$) and the *moderately strong* ($0.3 \leq W_r < 1 \text{ \AA}$) Mg II statistics conform to those derived from QSO surveys. In view of these new results we discuss possible explanations for the P06 result.

2. Data and Search Algorithm

The GRB afterglow sample comprises 8 echelle optical spectra ($R \equiv \lambda/\delta\lambda \approx 40\,000$ and $S/N > 5 \text{ pix}^{-1}$) taken with the Keck/HIRES (Vogt et al. 1994), Magellan/MIKE (Bernstein et al. 2003) and VLT/UVES (Dekker et al. 2000) spectrographs. This dataset comprises all current GRB echelle spectra available to our group. Table 1 lists the targets that we have used, along with references. Five of these spectra were used in the P06 survey (GRB021004, GRB050730, GRB050820, GRB051111, and GRB060418) and three are new (GRB050922C, GRB060607, and GRB080810). Note also that our survey extends beyond $z = 2$, while the P06 survey was restricted to $z \leq 2$. Data reduction was conducted in the same fashion as described in Tejos et al. (2007).

To identify Mg II systems in our sample we proceeded in two steps. We first performed a blind and automatic search for absorption lines using the "aperture method" (Wolfe et al. 1986; Churchill 2008). This yielded a list of lines detected at the 2.5σ confidence level. Mg II doublet candidates were searched for in this list by imposing a 5σ confidence limit on the stronger doublet $\lambda 2796$ line, but no constraint on the doublet ratio (DR) in order not to exclude blended lines.

The second step was to calculate EW values. To this end, we used direct pixel integration and, to conform to analysis techniques in QSO surveys (e.g., N07), complex systems were considered as a single one if the velocity span $\Delta v < 500 \text{ km s}^{-1}$. A careful inspection by eye allowed us to exclude spurious systems and obvious blends, and the final sample was built by imposing the criterion $1 < \text{DR} < 2$. This last condition did not exclude any possible system.

To test the sensitivity of our search algorithm we ran it over a sample of synthetic spectra of signal-to-noise ratio $S/N = 5$ and containing Mg II systems having a variety of column densities and Doppler parameters. This S/N ratio or better is representative of $\gtrsim 90\%$ of the redshift path, Δz . The efficiency was inferred by counting how many doublets were recovered over the total. The result of this analysis was that our detection method recovers 100% of the lines having $W_r^{2803} \geq 0.07 \text{ \AA}$ at this S/N level. Thus, for our survey we take $W_{min} = 0.07 \text{ \AA}$ in *both* components of the doublet. For this limit, the total redshift path is $\Delta z = 10.42$. The redshift-path density, $g(z)$, is shown in Figure 1.

3. Sample Definitions

We define following statistical samples:

Full Sample (FS) All Mg II systems between the redshifted Ly α and Mg II associated with the GRB, with $W_r^{2803} \geq 0.07 \text{ \AA}$ and detected at the 5σ and 2.5σ confidence level in $\lambda 2796$ and $\lambda 2803$, respectively. The Full Sample is composed of 23 Mg II systems (listed in Table 2). Note that we did not find any system with $W_r^{2803} > 0.07 \text{ \AA}$ in the GRB081010 spectrum and that Mg II-free sightlines are expected from QSO surveys.

Intervening Sample (IS) All systems in the FS but excluding those ones within 5000 km s^{-1} of z_{GRB} (labeled as 'Local' in Table 2). This sample is composed of 19 systems, having a median redshift of $\langle z \rangle = 1.4$. Figure 2 shows the velocity profiles of those systems with $W_r^{2796} < 1 \text{ \AA}$.

Strong Intervening Sample (SIS) All systems in the IS having $W_r^{2796} \geq 0.3 \text{ \AA}$. This is the same cutoff used in QSO absorption line surveys (e.g., Nestor et al. 2005, N07). This sample is composed of 14 systems (labeled as 'S' in Table 2) and is complete at the 99% level along a redshift path of $\Delta z = 10.86$. Systems with $W_r^{2796} \geq 1.0 \text{ \AA}$ are labeled with a 'V' (very strong) in the table. This latter limit is the same used by P06.

Weak Intervening Sample (WIS) All systems in the IS having $W_r^{2796} < 0.3 \text{ \AA}$. This sample is composed of 5 systems (labeled as 'W' in Table 2) and is complete at the 96% level over $\Delta z = 10.42$. The QSO absorption line survey we compare with was that one by N07. However, these authors were able to use the more sensitive limit $W_{min}^{2796} = 0.02 \text{ \AA}$. Consequently, for the sake of comparison between the GRB and QSO data, we recomputed $dN/dz|_{QSO}$ using a sub-sample drawn from their line list.

4. Results

Table 3 shows $dN/dz|_{GRB}$ (calculated in the same fashion as in Tejos et al. 2007) for 4 EW bins, along with $dN/dz|_{QSO}$ in the same bins. These numbers are plotted in Figure 3. At this point it is important to emphasize that, as in Tejos et al. (2007), our error estimation for the Poisson statistics is based on the tables given by Gehrels (1986) for small numbers. These errors are larger than the usual approximation, $\sigma_N = \sqrt{N}$.

From Figure 3 it is clear that our results for GRB sightlines match those ones for QSOs for equivalent widths $W_r^{2796} < 1 \text{ \AA}$, while for those with $W_r^{2796} \geq 1 \text{ \AA}$ we recover a similar overabundance as found by P06 which included low-resolution data.

In the WIS our result for GRB sightlines, $dN/dz|_{\text{GRB}}(\langle z \rangle = 1.4) = 0.48_{-0.21}^{+0.32}$, is consistent with $dN/dz|_{\text{QSO}}(\langle z \rangle = 1.2) = 0.71_{-0.10}^{+0.11}$ that we infer from the data presented by N07 (55 systems at $0.4 < z < 2.4$ having $W_r^{2803} \geq 0.07 \text{ \AA}$ and $W_r^{2796} < 0.3 \text{ \AA}$ in a total redshift path $\Delta z = 77.6^1$). We find that our central value is actually $\approx 70\%$ of the incidence estimated for QSO sightlines, but this difference is not significant. Therefore, we consider an overabundance of weak Mg II systems in GRB sightlines compared with that from QSOs to be very unlikely.

On the other hand, in the SIS we recover the result obtained by P06 for Mg II systems with $W_r^{2796} \geq 1 \text{ \AA}$, although we find an overabundance of a factor of 3 only, instead of 4, when comparing with the QSO results by Nestor et al. (2005). Because our redshift path is only two thirds that of P06, the significance of the result is reduced from 99.9% to $\approx 95.5\%$. Nonetheless, the fact that we have added new lines-of-sight argues that the GRB/QSO discrepancy is real, and possibly not due to statistical uncertainties nor a posteriori subtleties. However, note that both surveys have 5 spectra in common and are therefore not completely independent.

Finally, let us emphasize that there seems to be a transition at $W_r^{2796} \geq 1 \text{ \AA}$, as we see no significant GRB/QSO differences for intermediate EW values ($0.3 \text{ \AA} \leq W_r^{2796} < 1 \text{ \AA}$). This is more clearly seen in Figure 4, which shows the EW distribution in our GRB sample compared with previous parameterizations obtained from QSO samples (Nestor et al. 2005; Steidel & Sargent 1992).

5. Discussion and Implications

The fact that we do not find any discrepancy between the statistics of QSO and GRB weak Mg II systems opens the question as of why there is an overabundance of systems only for $W_r^{2796} > 1 \text{ \AA}$ systems in front of GRBs. Although the extant sample of afterglow spectra is still small, our result suggests that any explanation for the GRB/QSO discrepancy, be it intrinsic to the absorbers or a selection effect, should be inherent only to the galaxies that host strong absorbers in the line of sight to GRBs. In the following we discuss how the different models proposed to explain the P06 result may or may not be reinforced in light of our new results on weak systems.

¹The slightly different redshift coverage between the N07 data and ours makes no significant difference in this comparison.

Absorbers Intrinsic to the GRBs The present high-resolution spectra seem to rule out an intrinsic origin of the Mg II systems for two reasons. First, the line profiles, as seen at high spectral resolution, show no indication of broad and shallow absorption troughs, characteristic of BAL QSOs². Secondly, if some of the Mg II systems were intrinsic to the GRB, we would expect an overabundance also for the $W_r < 1 \text{ \AA}$ Mg II systems, which we do not observe (indeed, an overabundance of strong C IV would be expected too, and that is also not observed; Tejos et al. 2007).

GRB and QSO Beam Sizes The geometrical model proposed by Frank et al. (2007) (based on different GRB and QSO beam sizes, both comparable to the Mg II absorber characteristic sizes) has been tested and ruled out by subsequent observational analysis (Pontzen et al. 2007). Furthermore, initial claims of line-strength variability from Hao et al. (2007) in a single sightline (GRB060206) have been refuted (Thöne et al. 2008; Aoki et al. 2008). Nevertheless, we will consider this model in light of our new observations.

A consequence of the geometrical model (see Porciani et al. 2007) is that a fraction of weak systems in QSO spectra should have $DR \approx 1$. From the N07 sample we find this fraction to be $\approx 5\%$. Due to the smaller GRB beam sizes, the same fraction in GRB spectra is expected to be lower than this value. In contrast, we find that 2 out of 5 systems with $W_r^{2796} < 0.3 \text{ \AA}$ show $DR \approx 1$ (note that taking larger EW values would include saturated lines). Thus, this number, though not significant, does not support the geometrical model.

In addition, the model also predicts an underabundance of weak systems. This is suggested by our data for $W_r^{2796} < 0.3 \text{ \AA}$ systems, but the dN/dz values are consistent at the 1σ confidence level.

Dust As discussed in P06 and Porciani et al. (2007), the apparent high incidence of strong Mg II absorbers toward GRBs might be explained by an underestimated incidence of strong Mg II systems toward QSOs, as a consequence of sources that get lost due to dust obscuration. Although there is mounting counterevidence for a dust bias in QSO surveys (Ellison et al. 2001; Ellison & Lopez 2009; Ménard et al. 2008), from the point of view of the GRBs data alone our result on *weak* absorbers, a priori does not rule out the dust-obscuration scenario, at least qualitatively. This is so because dust is supposed not to have a considerable obscuring effect when $W_r < 1 \text{ \AA}$ (Ménard et al. 2008).

²However, we note that very shallow systems would not, in most cases, be detected in our GRB spectral sample.

On the other hand, a scenario where dust reduces the incidence of strong systems only in QSO sightlines is puzzling. In this scenario, the GRBs provide the unbiased (i.e., 'real') EW distribution but the observed EW distribution for GRBs is atypical (see Figure 4) when compared against any other line surveyed along QSO or GRB sightlines (e.g., C IV, Ly α ; Paschos et al. 2008). It seems that there is a transition at $W_r^{2796} \geq 1 \text{ \AA}$ where the EW distribution does not decrease as it would be expected. Therefore, in view of our new results, we conclude that dust is unlikely to explain the differences between Mg II toward QSO and GRB sightlines.

Gravitational Lensing Source amplification due to strong gravitational lensing may bias the GRB spectral samples toward targets that contain more intervening absorbers, if these occur in the lensing galaxies (P06; Porciani et al. 2007). Our spectral sample does not offer a direct means to infer what kind of Mg II systems may be associated to galaxy configurations being more or less lensing-efficient. Obviously, further deep late-time imaging observations of GRB fields (e.g., Chen et al. 2009) must be carried out in order to identify the absorbing galaxies and possibly look for impact-parameter/line-strength correlations.

Nevertheless, if we speculate that the strong absorber overdensity is purely explained by a selection effect due to lensing magnification, our results can help us estimate the fraction f_l of magnified GRBs that otherwise would not have been spectroscopically observed. To estimate f_l , let us consider a Mg II survey composed by M QSO sightlines. Then, the expected number of absorption systems will be:

$$N_{QSO} = \frac{dN}{dz}_{QSO} \langle \Delta z \rangle M ,$$

where $\langle \Delta z \rangle$ is the average redshift path per sightline and $dN/dz|_{QSO}$ is the expected incidence of systems (assumed unbiased; a quantitative detail of a possible lensing bias in QSO surveys is beyond the scope of this paper).

Let us now consider an equivalent GRB survey with M sightlines. If the observed number of absorption systems, N_{GRB} , is a factor of e greater than N_{QSO} , then the excess of systems will be $N_e = N_{QSO}(e - 1)$. Let L be the total number of lensed sightlines in that GRB survey. The fraction of magnified GRBs is then:

$$f_l \equiv \frac{L}{M} .$$

If we assume that the excess of systems is just due to lensing (either macro or microlensing³), then any extra system corresponds to a lensed sightline:

$$L = N_e ,$$

and therefore:

$$f_l = (e - 1) \frac{dN}{dz}_{QSO} \langle \Delta z \rangle .$$

Thus, in order to reproduce the factor of ≈ 3 enhancement that is observed at this EW level, we estimate that f_l must be of the order of $\approx 60\%$ ($e \approx 3$, $dN/dz|_{QSO} \approx 0.3$ and $\langle \Delta z \rangle \approx 1$). Such a fraction would add twice as many strong systems as encountered if there were no lensing⁴. Similarly, an enhancement factor of ≈ 2 (still consistent with our result at the 1σ c.l.) would require $f_l \approx 30\%$. Since more realistically $L \leq N_e$, this estimate of f_l should be taken as an upper limit. Note that we do not provide here a quantitative assessment of the lensing magnification but instead we assume that it is large enough to provide $f_l > 0$. In fact, in the above situation our results would imply that the lensing agents contribute only systems with $W_r \geq 1 \text{ \AA}$ (where $e > 1$; note that this could be easily explained if weak absorbers were indeed more external to galaxies, as proposed by N07 among others). In summary, we believe that lensing by the galaxies hosting strong absorbers provides a viable explanation to the QSO/GRB discrepancy (see also Vergani et al. 2009).

A test of the lensing hypothesis could be made with very rapid and deep spectroscopy of 'dark' bursts (e.g., Perley et al. 2009), for which $dN/dz|_{GRB}$ should show no enhancement. In addition, as mentioned above, another test of this bias is that there should be more massive (and more luminous) intervening galaxies at low impact parameters in sightlines where the Mg II EW is larger.

³The optical depth for microlensing increases at low impact parameters from galaxies (the surface density of stars and MACHOs is greater in the center than in the outskirts of galaxies) therefore it should also contribute to the excess of strong systems (see also Porciani et al. 2007).

⁴Note that this argument becomes unrealistic for a factor of ≈ 4 enhancement, for which f_l would approach $\approx 100\%$.

6. Summary

We have used echelle spectra of 8 GRB afterglows, three of them new, to show that the incidence of weak Mg II systems ($0.07 \text{ \AA} \leq W_r^{\text{MgII}} < 1 \text{ \AA}$) is the same as toward QSO lines of sight. There seems to be a transition at $W_r \approx 1 \text{ \AA}$, above which $dN/dz|_{\text{GRB}}$ rises significantly to a factor of a few with respect to $dN/dz|_{\text{QSO}}$, as found by P06. In view of the present results on weak absorbers, we suggest that the GRB/QSO discrepancy should arise in the galaxies that host the strong absorbers. Effects associated to the GRB phenomenon like ejected absorbers or different beam-sizes are not supported by the data presented here nor a selection effect due to dusty absorbers. Instead, of all effects proposed in the literature, a bias toward sources amplified by lensing seems to be in best agreement with our findings.

This paper includes data obtained through the Gamma-ray Bursts Afterglows as Probes (GRAASP) Collaboration (<http://www.graasp.org>) from the following observatories: the W. M. Keck Observatory, which is a joint facility of the University of California, CIT, and NASA, and the 6.5 m Magellan Telescopes located at Las Campanas Observatory, Chile. This paper also includes data based on observations made with ESO Telescopes at the Paranal Observatories under programs 070.A-0599(B), 075.A-0603(B) and 077.D-0661(A). SL and NT are partly supported by the Chilean *Centro de Astrofísica* FONDAF No. 15010003, and by FONDECYT grant N°1060823. JXP is partially supported by NASA/Swift grant NNG05GF55G and an NSF CAREER grant (AST-0548180).

Table 1. GRB Spectral Sample.

Source	RA (J2000)	Dec (J2000)	z_{GRB}	Δz^a	Instrument	Reference
GRB021004	00 26 54.68	+18 55 41.6	2.335	1.55	UVES	1
GRB050730	14 08 17.14	−03 46 17.8	3.969	1.14	MIKE	2,3
GRB050820	22 29 38.11	+19 33 37.1	2.615	1.10	HIRES	3
GRB050922C	21 09 33.30	−08 45 27.5	2.199	1.56	UVES	4
GRB051111	23 12 33.36	+18 22 29.5	1.549	0.93	HIRES	3
GRB060418	15 45 42.40	−03 38 22.8	1.490	1.18	MIKE	3
GRB060607	21 58 50.40	−22 29 46.7	3.082	1.61	UVES	5
GRB080810	23 47 10.40	+00 19 11.0	3.35	1.40	HIRES	6,7

Note. — ^a Individual redshift path for our Mg II Intervening Sample (see definition in §3).

References. — (1) Fiore et al. (2005); (2) Chen et al. (2005); (3) Prochaska et al. (2007); (4) Piranomonte et al. (2006); (5) Ledoux et al. (2006); (6) Prochaska et al. (2008); (7) Page et al. (2008).

Table 2. Full Sample (FS) of Mg II in GRB Spectra

GRB	z_{GRB}	z_{start}	$z_{end}^{\beta c=5000km\ s^{-1}}$	z_{abs}^{MgII}	$W_r^{pixel}(2796)$ $W_r^{pixel}(2803)$	DR	Comment ^a	
021004	2.335	0.44795	2.27938	0.56446	0.140 ± 0.013	1.085 ± 0.155	W	
					0.129 ± 0.014			
					1.38067	1.633 ± 0.016	1.251 ± 0.023	VS
						1.305 ± 0.020		
					1.60274	1.389 ± 0.026	1.227 ± 0.025	VS
						1.132 ± 0.010		
050730	3.97	1.5781	3.88711	1.77317	2.29920	0.335 ± 0.016	1.701 ± 0.139	S
						0.197 ± 0.013		
					2.32893	0.814 ± 0.078	1.040 ± 0.108	Local
						0.783 ± 0.032		
					050730	0.923 ± 0.019	1.165 ± 0.038	S
						0.792 ± 0.020		
050820	2.6147	0.5694	2.55441	0.69153	2.25378	1.125 ± 0.034	1.426 ± 0.087	VS
						0.789 ± 0.042		
					050820	2.988 ± 0.022	1.280 ± 0.017	VS
	2.335 ± 0.025							
	1.43000	VS				
	1.62040	1.262 ± 0.016	...	W				
	...							
050922C	2.199	0.3889	2.14565	1.10731	0.532 ± 0.031	1.482 ± 0.119	S	
						0.359 ± 0.020		
				2.19950	1.062 ± 0.058	0.700 ± 0.041	Local	
					1.518 ± 0.035			
051111	1.549	0.1067	1.50649	0.82735	0.369 ± 0.010	1.242 ± 0.060	S	
						0.297 ± 0.012		
					1.18910	2.091 ± 0.011	1.201 ± 0.009	VS
					1.741 ± 0.010			
				1.54913	2.343 ± 0.010	1.106 ± 0.007	Local	
					2.118 ± 0.010			
060418	1.49	0.0811	1.44847	0.60259	1.299 ± 0.015	1.054 ± 0.018	VS	
						1.233 ± 0.015		
					0.65593	0.975 ± 0.010	1.237 ± 0.021	S
						0.788 ± 0.011		
					1.10724	1.832 ± 0.020	1.222 ± 0.019	VS
	1.499 ± 0.017							
	1.32221	0.214 ± 0.009	1.609 ± 0.139	W				
		0.133 ± 0.010						
		1.48964	1.968 ± 0.017	1.150 ± 0.015	Local			
			1.711 ± 0.017					
060607	3.082	0.7723	3.01392	1.51057	0.197 ± 0.010	1.698 ± 0.183	W	
						0.116 ± 0.011		
					1.80208	1.906 ± 0.011	1.228 ± 0.015	VS
						1.552 ± 0.016		
	2.27840	0.293 ± 0.015	1.024 ± 0.080	W				

Table 2—Continued

GRB	z_{GRB}	z_{start}	$z_{end}^{\beta c=5000 km s^{-1}}$	z_{abs}^{MgII}	$W_r^{pixel}(2796)$ $W_r^{pixel}(2803)$	DR	Comment ^a
080810	3.35	0.107	3.277	...	0.286 ± 0.017	

Note. — All Mg II absorption systems between the redshifted Ly α and Mg II associated with the GRB. We did not find any system having $W_r^{2803} > 0.07 \text{ \AA}$ in the GRB081010 spectrum.

^a See notation defined in §3.

Table 3. Incidence of Intervening Mg II Absorption Systems toward GRBs

$W_r [\text{\AA}]$	N_{abs}	Δz	$\langle z \rangle$	$dN/dz _{GRB}$	$dN/dz _{QSO}^{MgII} \text{ }^a$
$0.07 \leq W_r^{2803}$ and $W_r^{2796} < 0.3$	5	10.42	1.46	$0.48^{+0.32}_{-0.21}$	$0.71^{+0.11}_{-0.10}$
$0.3 \leq W_r^{2796} < 0.6$	3	10.80	1.41	$0.28^{+0.27}_{-0.15}$	0.29 ± 0.04
$0.6 \leq W_r^{2796} < 1.0$	2	10.86	1.22	$0.18^{+0.24}_{-0.12}$	0.21 ± 0.02
$1.0 \leq W_r^{2796}$	9	10.86	1.34	$0.83^{+0.38}_{-0.27}$	0.28 ± 0.01

Note. — ^a Values in this column were calculated from N07 ($W_r < 0.3 \text{ \AA}$) and Nestor et al. (2005) ($W_r \geq 0.3 \text{ \AA}$). Since no redshift list is available in Nestor et al. (2005), we calculated dN/dz assuming similar redshift coverage and $\frac{dN}{dz}(W_r^a < W_r < W_r^b) = \frac{dN}{dz}(W_r^a < W_r) - \frac{dN}{dz}(W_r^b < W_r)$.

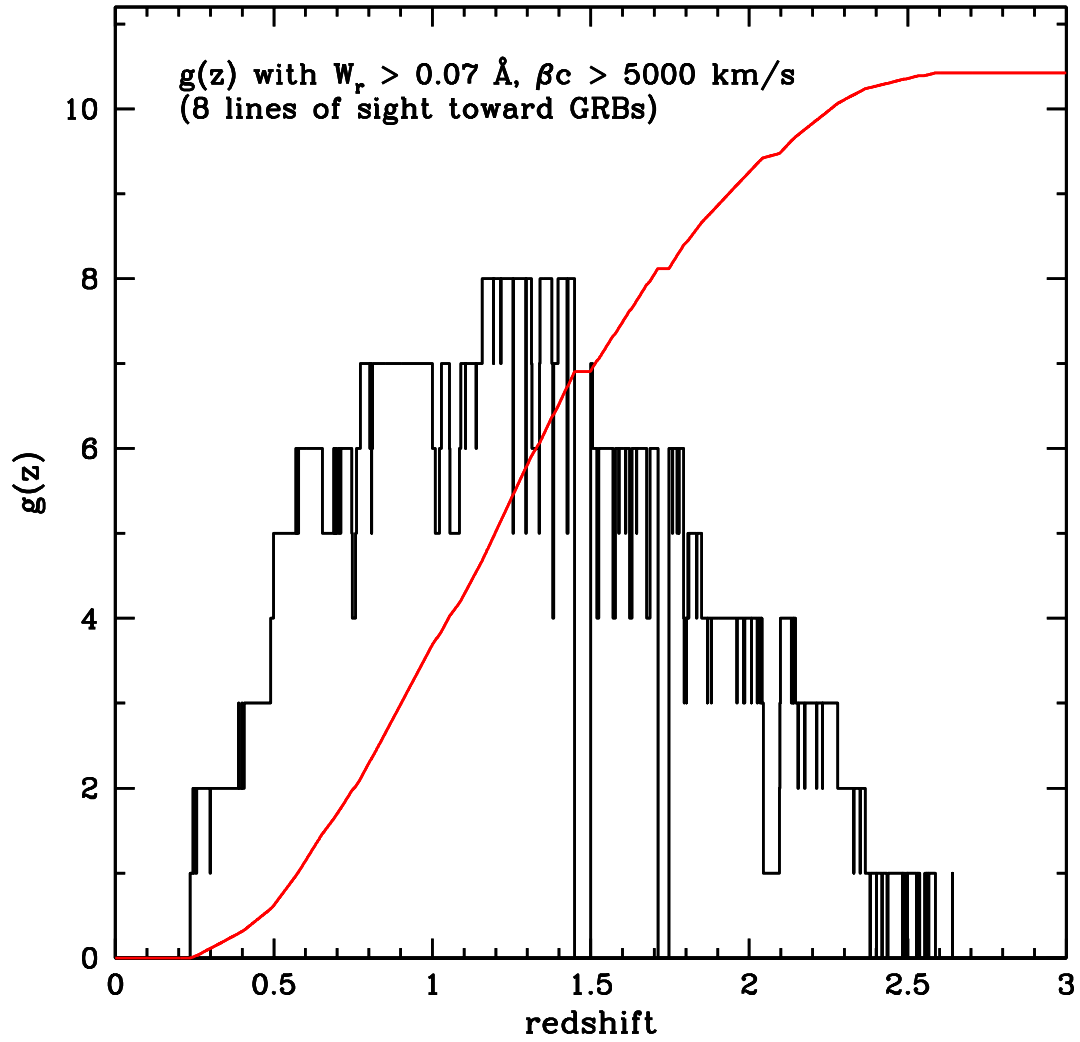


Fig. 1.— Number of lines of sight in the Mg II survey and cumulative redshift path as a function of redshift for $W_{min} = 0.07 \text{ \AA}$.

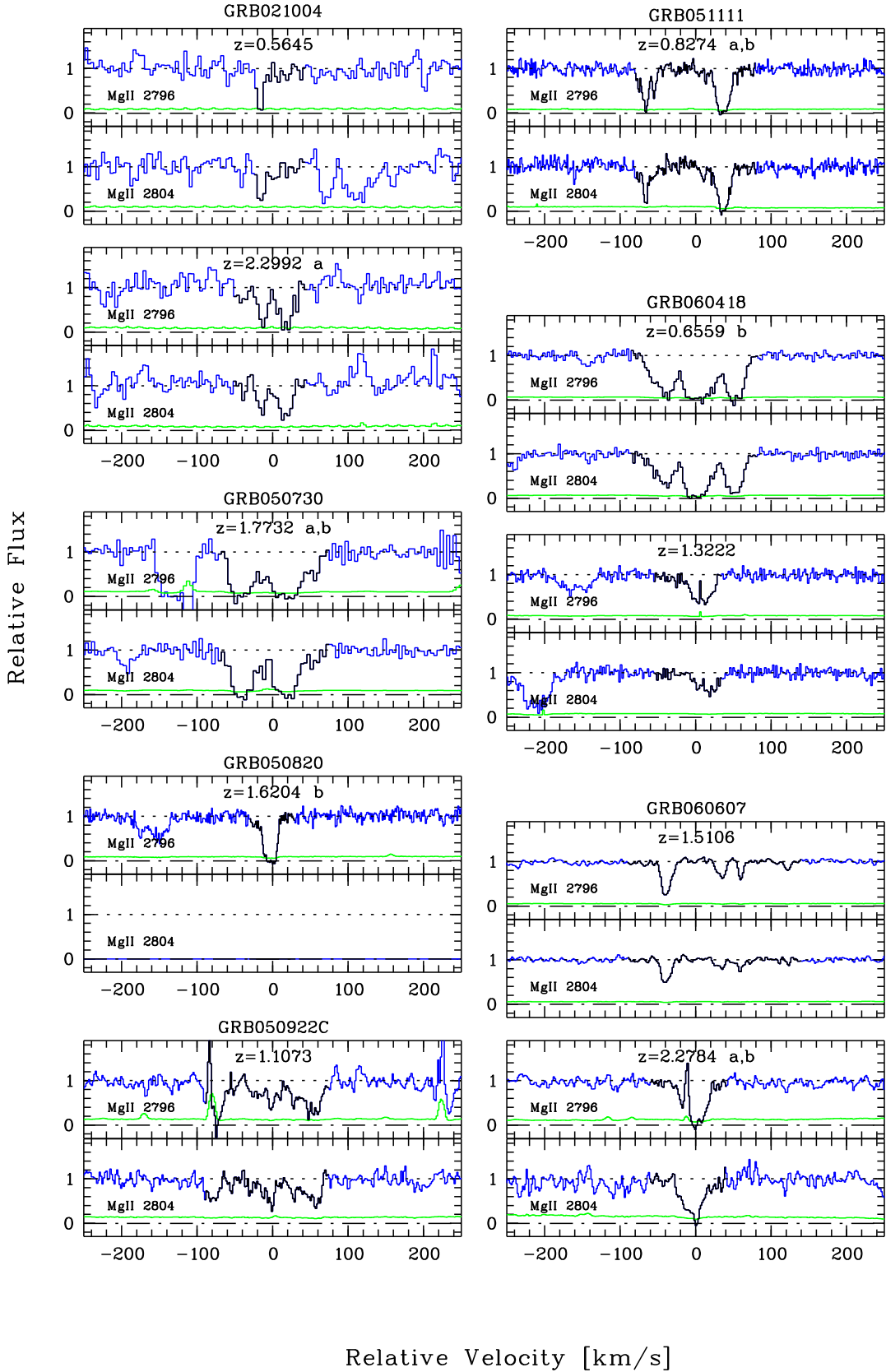


Fig. 2.— Velocity profiles of intervening Mg II systems with $W_r^{2796} < 1.0 \text{ \AA}$. The labels to the right of the redshifts indicate a Mg I ('a') or Fe II ('b') detections

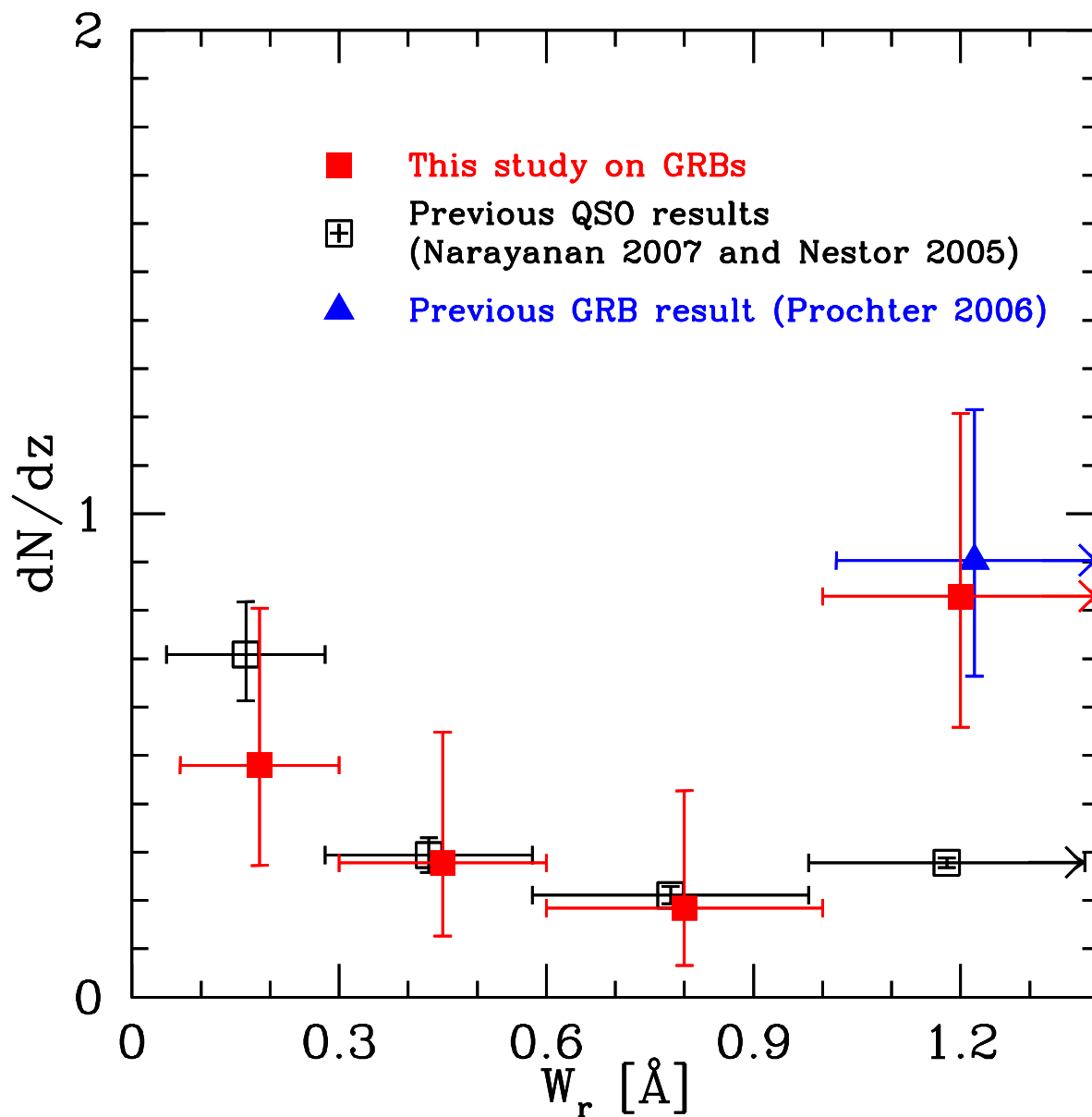


Fig. 3.— Redshift number density of Mg II absorption systems toward GRB afterglows (filled squares; see the numbers in Table 3). Empty squares (slightly offset in x for the sake of clarity) depicts the QSO results from N07 ($W_r^{2796} < 0.3 \text{ \AA}$) and Nestor et al. (2005) [$W_r^{2796} \geq 0.3 \text{ \AA}$]. The triangle indicates the P06 result for GRBs. Note that both surveys have 5 spectra in common and are therefore not completely independent. Also note that the high EW bin corresponds to $W_r^{2796} \geq 1 \text{ \AA}$.

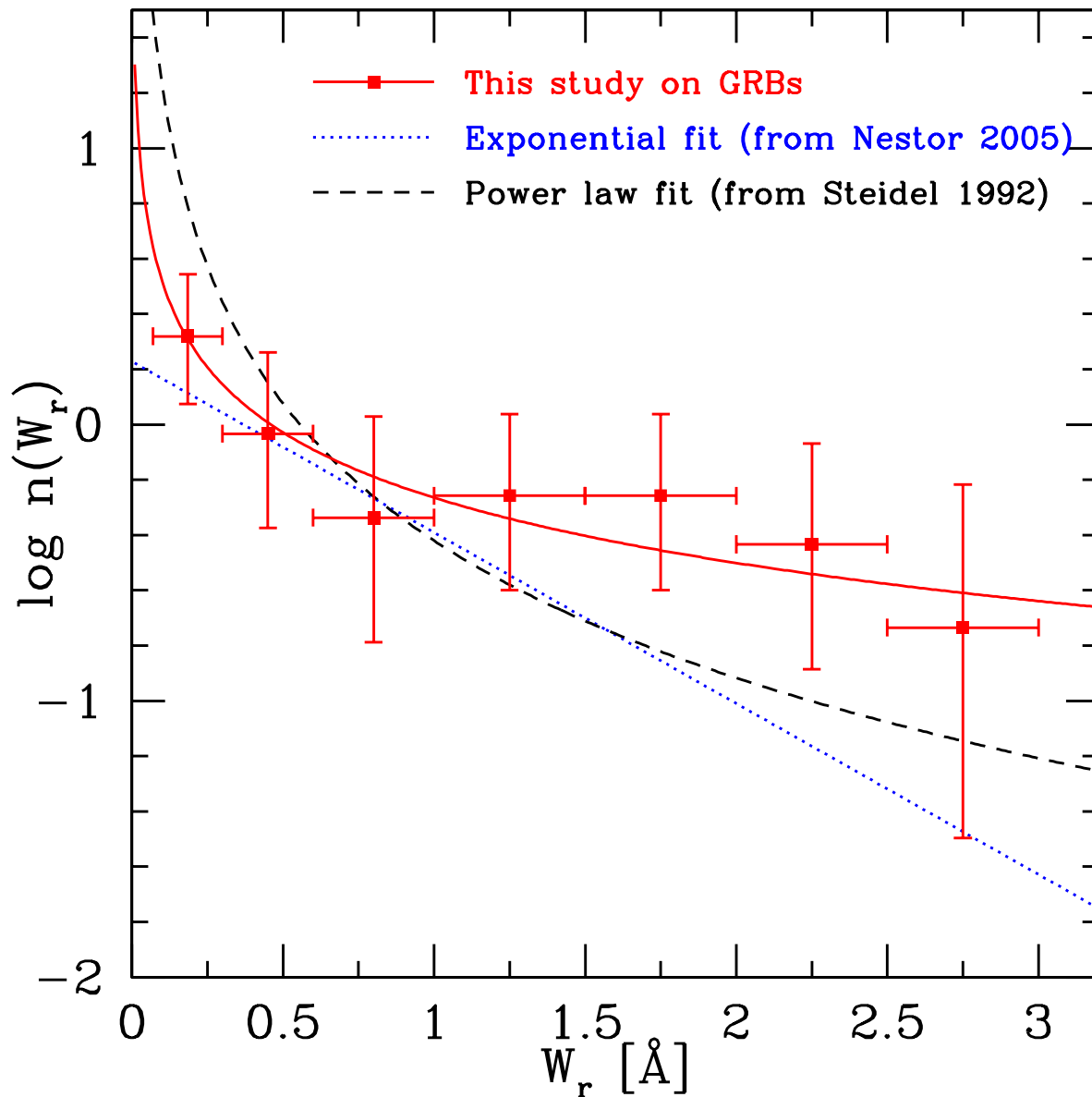


Fig. 4.— Equivalent width distribution of Mg II absorption systems toward GRB afterglows (filled squares). The solid line corresponds to the best-fit power-law to the data points. The dotted and dashed lines correspond to the expected distributions from QSO sightlines: an exponential fit for systems at $W_r^{2796} \geq 0.3 \text{ \AA}$ (dotted line; from Nestor et al. 2005) and a power-law fit for systems at $W_r^{2796} < 0.3 \text{ \AA}$ (dashed line; from Steidel & Sargent 1992).

REFERENCES

- Aoki, K., et al. 2008, arXiv:0808.4157
- Bernstein, R., Shectman, S. A., Gunnels, S. M., Mochnacki, S., & Athey, A. E. 2003, Proc. SPIE, 4841, 1694
- Chen, H.-W., Prochaska, J. X., Bloom, J. S., & Thompson, I. B. 2005, ApJ, 634, L25
- Chen, H.-W., et al. 2009, ApJ, 691, 152
- Churchill, C. W., Rigby, J. R., Charlton, J. C., & Vogt, S. S. 1999, ApJS, 120, 51
- Churchill, C. 2008, QSO Absorption Lines Studies: Ultraviolet and Optical Spectroscopy
- Cucchiara, A., Jones, T., Charlton, J. C., Fox, D. B., Einsig, D., & Narayanan, A. 2008, arXiv:0811.1382
- Dekker, H., D’Odorico, S., Kaufer, A., Delabre, B., & Kotzlowski, H. 2000, Proc. SPIE, 4008, 534
- Ellison, S. L., Yan, L., Hook, I. M., Pettini, M., Wall, J. V., & Shaver, P. 2001, A&A, 379, 393
- Ellison, S. L., & Lopez, S. 2009, arXiv:0904.3330
- Fiore, F., et al. 2005, ApJ, 624, 853
- Frank, S., Bentz, M. C., Stanek, K. Z., Mathur, S., Dietrich, M., Peterson, B. M., & Atlee, D. W. 2007, Ap&SS, 312, 325
- Gehrels, N. 1986, ApJ, 303, 336
- Hao, H., et al. 2007, ApJ, 659, L99
- Kann, D. A., Klose, S., & Zeh, A. 2006, ApJ, 641, 993
- Ledoux, C., Vreeswijk, P., Smette, A., Jaunsen, A., & Kaufer, A. 2006, GRB Coordinates Network, 5237, 1
- Ménard, B., Nestor, D., Turnshek, D., Quider, A., Richards, G., Chelouche, D., & Rao, S. 2008, MNRAS, 385, 1053
- Milutinović, N., Rigby, J. R., Masiero, J. R., Lynch, R. S., Palma, C., & Charlton, J. C. 2006, ApJ, 641, 190

- Narayanan, A., Misawa, T., Charlton, J. C., & Kim, T.-S. 2007, *ApJ*, 660, 1093 (N07)
- Nestor, D. B., Turnshek, D. A., & Rao, S. M. 2005, *ApJ*, 628, 637
- Olivares, F., Kruehler, T., Greiner, J., & Filgas, R. 2009, GRB Coordinates Network, 9215
- Page, K. L., et al. 2008, GRB Coordinates Network, 8080, 1
- Paschos, P., Jena, T., Tytler, D., Kirkman, D., & Norman, M. L. 2008, arXiv:0802.3730
- Perley, D. A., et al. 2009, arXiv:0905.0001
- Piranomonte, S., D’Elia, V., Ward, P., Fiore, F., & Meurs, E. J. A. 2006, *Nuovo Cimento B Serie*, 121, 1561
- Pollack, L. K., Chen, H. ., Prochaska, J. X., & Bloom, J. S. 2009, ArXiv e-prints
- Pontzen, A., Hewett, P., Carswell, R., & Wild, V. 2007, *MNRAS*, 381, L99
- Porciani, C., Viel, M., & Lilly, S. J. 2007, *ApJ*, 659, 218
- Prochaska, J. X., et al. 2007, *ApJS*, 168, 231
- Prochaska, J. X., Chen, H.-W., Dessauges-Zavadsky, M., & Bloom, J. S. 2007, *ApJ*, 666, 267
- Prochaska, J. X., Perley, D., Howard, A., Chen, H.-W., Marcy, G., Fischer, D., & Wilburn, C. 2008, GRB Coordinates Network, 8083
- Prochter, G. E., et al. 2006, *ApJ*, 648, L93 (P06)
- Savaglio, S. 2006, *New Journal of Physics*, 8, 195
- Steidel, C. C., & Sargent, W. L. W. 1992, *ApJS*, 80, 1
- Sudilovsky, V., Savaglio, S., Vreeswijk, P., Ledoux, C., Smette, A., & Greiner, J. 2007, *ApJ*, 669, 741
- Sudilovsky, V., Smith, D., & Savaglio, S. 2009, arXiv:0904.3227
- Tanvir N., et al. 2009, GRB Coordinates Network, 9219
- Tejos, N., Lopez, S., Prochaska, J. X., Chen, H.-W., & Dessauges-Zavadsky, M. 2007, *ApJ*, 671, 622
- Thöne, C. C., et al. 2008, *A&A*, 489, 37

Vergani, S. D., Petitjean, P., Ledoux, C., Vreeswijk, P., Smette, A., & Meurs, E. J. A. 2009, *A&A*, 503, 771

Vreeswijk, P. M., et al. 2004, *A&A*, 419, 927

Vogt, S. S., et al. 1994, *Proc. SPIE*, 2198, 362

Wolfe, A. M., Turnshek, D. A., Smith, H. E., & Cohen, R. D. 1986, *ApJS*, 61, 249